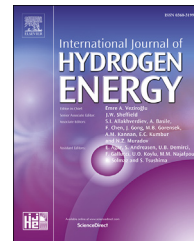


Available online at www.sciencedirect.com**ScienceDirect**journal homepage: www.elsevier.com/locate/he

Study of a double fed induction generator using matrix converter: Case of wind energy conversion system

K. Bedoud ^{a,c,*}, A. Rhif ^b, T. Bahi ^c, H. Merabet ^a

^a Research Center in Industrial Technologies CRTI, ex CSC, BP 64 Cheraga, Algeria

^b Laboratory of Advanced Systems (Polytechnic School of Tunisia), University of Carthage, Tunisia

^c Automatic Laboratory and Signals, Badji Mokhtar University, Annaba, Algeria

ARTICLE INFO

Article history:

Received 15 April 2017

Accepted 2 July 2017

Available online xxx

Keywords:

Wind turbine

Control

Maximum power tracking

Matrix converter

Doubly fed induction generator

ABSTRACT

Due to the growing of the power electronics, especial attention has been given to the use of new generation of power converters, AC/AC matrix converter to which provide a direct power converter AC/AC, bi-directional power flow, almost sinusoidal input and output waveform. In this paper, we present the performance study of a variable-speed wind turbine based on doubly fed induction generator fed by matrix converter using the maximum power point tracking method to extract the maximum power available. The whole system is presented in d-q-synchronous reference frame. The control scheme is tested and the performances are evaluated by simulation results. The simulation results obtained under MatLab/Simulink show the effectiveness and validity of the considered control.

© 2017 Hydrogen Energy Publications LLC. Published by Elsevier Ltd. All rights reserved.

Introduction

Starting from the principle of Lavoisier: Nothing is lost, nothing is created, everything is transformed. Energy is the motor of natural phenomena, it can be transformed from one form to another. Wind energy is one of the cleanest sources of energy because while producing electricity it does not generate any gas greenhouse effect, does not degrade air quality and does not pollute soils or water. Furthermore, it does not produce toxic or radioactive waste [1–5]. Nowadays, Owing to the increasing pollution of environment and atmosphere, huge efforts have been made in promoting the wind energy conversion systems WECS to reduce costs and increase reliability and robustness [6]. Indeed, it exists several WECS

which allow transforming the wind kinetic energy into electrical energy. In this work, the WECS is constituted, principally, of a turbine, a gearbox and a doubly fed induction generator (DFIG). The DFIG is connected directly to the grid via its stator but also via its rotor by means of matrix converter (MC) to allow an exchange of energy between the network and the DFIG at the synchronism speed. Wind turbine is a mechanical device, it ensures the conversion of the kinetic energy into mechanical energy, there after it will be converted to electrical energy by coupling a generator to the wind turbine. Nowadays, in the field of renewable energies, several types of electric machines are used as generators in wind energy conversion systems [6–8]. Therefore, the study of double fed induction generator (DFIG) has regained importance because it has become the most popular generators for wind energy

* Corresponding author. Research Center in Industrial Technologies CRTI, ex CSC, BP 64 Cheraga, Algeria.

E-mail addresses: k.bedoud@crti.dz, khoulou1981@yahoo.fr (K. Bedoud).

<http://dx.doi.org/10.1016/j.ijhydene.2017.07.010>

0360-3199/© 2017 Hydrogen Energy Publications LLC. Published by Elsevier Ltd. All rights reserved.

applications. The converter consists of nine bi-directional switches, arranged as three sets of three so that any of the three input phases can be connected to any of the three output lines. There is now competition between the matrix converter and the voltage source inverter with a regenerative input rectifier [9]. The MC is widely used in large wind farms, and this for its many advantages: direct power converter AC/AC, bi-directional power flow, quasi sinusoidal input and output waveform, and allows to control: the rotor currents magnitude, frequency and input power factor [10–12]. Moreover, the use of matrix converter instead of two converters allow the reduce of maintenance, cost and number of components used in conventional systems [13]. The wind turbine can be operated at the maximum power operating point (MPPT) for various wind speeds by adjusting the shaft speed optimally to achieve maximum efficiency at all wind velocities [14–16]. Pitch angle regulation is required in conditions above the rated wind speed when the rotational speed is not kept constant. Small changes in pitch angle can have a dramatic effect on the power output [17].

The aim of this work is to show the importance of wind energy conversion system (WECS) driven by matrix converter.

This paper is organized as follows, in Section [Wind system modeling](#), the modeling of the turbine and gearbox is presented. In Section [Control structure](#), firstly, the mathematical model of doubly fed induction generator is given, then, the model of three phases converter matrix and its control strategy are considered. The whole of the chain studied and completed by the necessary details are established in Section [Simulation results](#). In Section [Conclusion](#), computer simulation results obtained under MatLab/Simulink are shown and discussed. Finally, the reported work is concluded.

Wind system modeling

The wind energy conversion system considered in this work includes the wind turbine, gearbox, double fed induction generator, matrix converter and the electrical network. [Fig. 1](#) shows the equivalent diagram of wind energy conversion systems.

Wind turbine modeling

The mechanical power produced by the wind is given by Refs. [13,18]:

$$P_{tur} = C_p(\lambda, \beta) \cdot \frac{\rho \cdot S \cdot V^2}{2} \quad (1)$$

The power coefficient of wind turbine $C_p(\lambda, \beta)$ can be defined as a function of the blade pitch angle (β) and the tip-speed ratio (λ) which is given by Refs. [13,19–21]:

$$\lambda = \frac{R \cdot \Omega_{tur}}{V} \quad (2)$$

C_p is different from a turbine to another, and is usually provided by the manufacturer and can be used to define a mathematical approximation. Generally, the used expression of the power coefficient can be approximated by the following Eqs. (22) and (23):

$$C_p(\lambda, \beta) = 0.22 \left(\frac{116}{\lambda_i} - 0.4\beta - 5 \right) e^{-\frac{12.5}{\lambda_i}} \quad (3)$$

$$\frac{1}{\lambda_i} = \frac{1}{\lambda + 0.08\beta} - \frac{0.035}{1 + \beta^3} \quad (4)$$

So, the aerodynamic torque is expressed by Refs. [13,22]:

$$T_{tur} = \frac{P_{tur}}{\Omega_{tur}} = C_p(\lambda, \beta) \cdot \frac{\rho \cdot S \cdot V^3}{2} \cdot \frac{1}{\Omega_{tur}} \quad (5)$$

Modeling of the mechanical part

[Fig. 2](#) show the mechanical part of the wind turbine. The gearbox is installed between the turbine and the generator to adapt the turbine speed to that of the generator. Thus, we define the mathematical expressions of the chain as follows [24]:

$$\Omega_{mec} = G \cdot \Omega_{tur} \quad (6)$$

Furthermore, In the case where: friction, elasticity and energy losses in the gearbox are neglected.

$$G = \frac{T_{tur}}{T_{mec}} \quad (7)$$

The mechanical equations of the system can be characterized by:

$$J \frac{d\Omega_{mec}}{dt} = T_{mec} - T_{em} - f\Omega_{mec} \quad (8)$$

with: $J = \frac{J_{tur}}{G^2} + J_{gen}$

[Fig. 3](#) show the block diagram of the wind turbine shaft model associated with the turbine model.

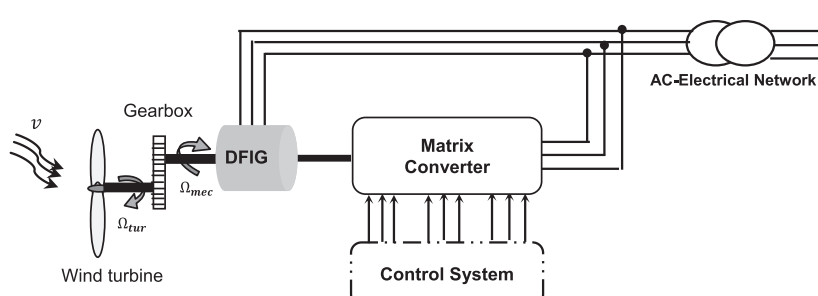


Fig. 1 – Block diagram of wind energy conversion system.

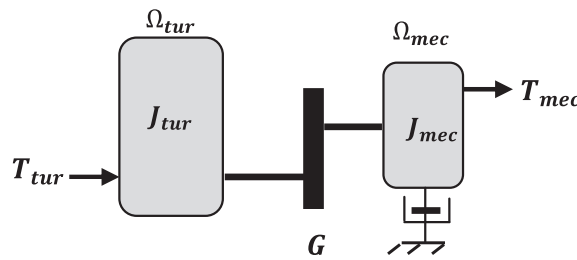


Fig. 2 – Mechanical part of wind turbine.

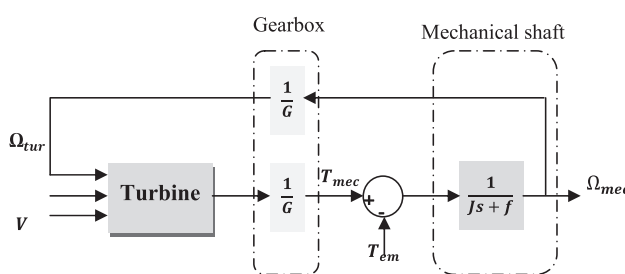


Fig. 3 – Wind turbine model.

Based on the mathematical expressions programming of the model previously developed, Fig. 4 exposes the computed relation between the power coefficient C_p and the tip-speed ratio λ for different blade pitch β using wind turbine parameters given in the appendix. The power extracted from the wind is maximized when the power coefficient is optimal C_{popt} . Therefore, we must set the tip speed ratio on its optimal value λ_{opt} . For each wind speed, the machine rotates so that it captures the maximum available power. Based on previous relationships, the Power-Velocity characteristic can be plotted for different wind speeds (see Fig. 5). From this figure we may

notice that there is one specific point $(\lambda_{opt}, C_{popt})$ which ensures the maximum power captured from the wind for each pitch angle.

Fig. 6 summarizes the rotational speeds Ω_{mec} calculated as a function of the optimal tip speed ratio λ_{opt} value for different blade pitch angle. These speeds allow extracting maximum powers.

Modeling of the DFIG

DFIG model is presented in synchronous dq reference frame. The d-axis is aligned with the stator flux linkage vector φ_s , and then, $(\varphi_{sq} = 0, \varphi_{sd} = \varphi_s)$ [18,25]. Considering that the resistance of the stator winding (R_s) is neglected and the grid is supposed stable with voltage (v_s) and synchronous angular frequency (ω_s) constant what implies $\varphi_{sd} = cst$, the stator voltage equations windings can be simplified in steady state as [5]:

$$\begin{cases} V_{sd} = \frac{d\varphi_{sd}}{dt} = 0 \\ V_{sq} = \omega_s \cdot \varphi_{sd} = V_s \end{cases} \quad (9)$$

Hence, the DFIG mathematical model can be written as follow:

$$\begin{cases} V_{sd} = \frac{R_s}{L_s} \varphi_{sd} - \frac{R_s}{L_s} L_m i_{rd} \\ V_{sq} = -\frac{R_s}{L_s} L_m i_{rq} + \omega_s \varphi_{sd} \end{cases} \quad (10)$$

$$\begin{cases} V_{rd} = R_r i_{rd} + \sigma \cdot L_r \frac{di_{rd}}{dt} + e_{rd} \\ V_{rq} = R_r i_{rq} + \sigma \cdot L_r \frac{di_{rq}}{dt} + e_{rq} + e_\varphi \end{cases} \quad (11)$$

$$\begin{cases} \varphi_{rd} = \left(L_r - \frac{M^2}{L_s} \right) i_{rd} + \frac{MV_s}{\omega_s L_s} \\ \varphi_{rq} = \left(L_r - \frac{M^2}{L_s} \right) i_{rq} \end{cases} \quad (12)$$

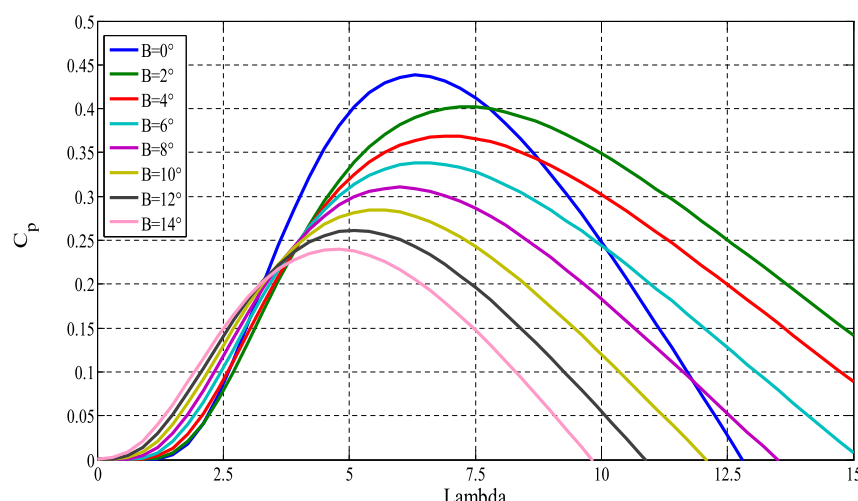


Fig. 4 – Power coefficient characteristics.

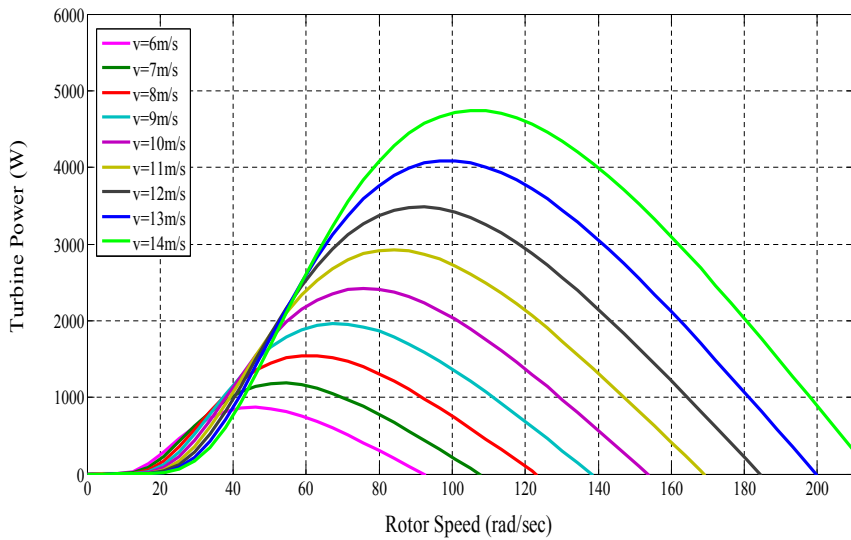


Fig. 5 – Turbine power characteristics.

$$\left\{ \begin{array}{l} P_s = -\frac{V_s \cdot M}{L_s} \cdot i_{rq} \\ Q_s = \frac{V_s^2}{L_s \omega_s} - \frac{M \cdot V_s}{L_s} \cdot i_{rd} \\ P_r = g \cdot \frac{V_s \cdot M}{L_s} \cdot i_{rq} \\ Q_r = g \cdot \frac{V_s \cdot M}{L_s} \cdot i_{rd} \end{array} \right. \quad (13)$$

with:

$$\left\{ \begin{array}{l} e_{rd} = -\sigma \cdot L_r \cdot \omega_r \cdot i_{rq} \\ e_{rq} = \sigma \cdot L_r \cdot \omega_r \cdot i_{rd} \\ e_\varphi = \omega_r \cdot \frac{M}{L_s} \cdot \varphi_{sd} \\ \sigma = 1 - \left(\frac{M}{\sqrt{L_s L_r}} \right)^2 \end{array} \right. \quad (14)$$

From Eq. (13), we can deduce that the active and reactive powers can reach decoupling control. The electromagnetic torque is as follows [22]:

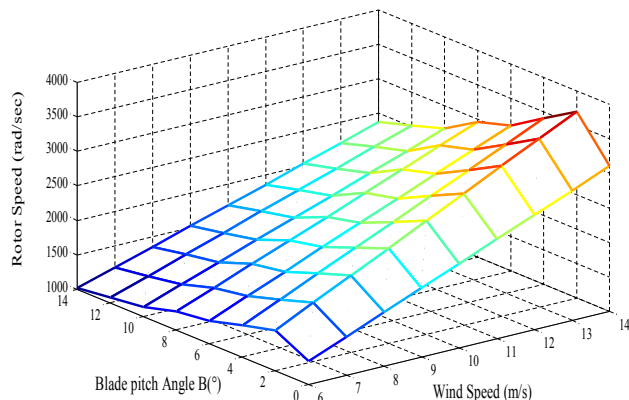


Fig. 6 – Presentation of lookup table data for WEC system.

$$T_{em} = 3P \cdot \frac{M}{2} (i_{rd} \cdot i_{sq} - i_{rq} \cdot i_{sd}) \quad (15)$$

Modeling and control of matrix converter

The MC studied in this paper is 9×3 bidirectional switch single pole power converter. It is used to convert nine AC phase input voltage into three AC phase output, with a control of magnitude and frequency current output. Venturini algorithm is used to control 27 switches of $2^{3 \times 3}$ combinations Dependent on the semiconductor switching states of the matrix converter [26,27]. The MC structure is shown in Fig. 7.

The three phase output voltages (V_a , V_b , V_c) are represented in terms of input voltages (V_A , V_B , V_C) as follows [23–28]:

$$\begin{bmatrix} V_a \\ V_b \\ V_c \end{bmatrix} = \begin{bmatrix} S_{Aa} & S_{Ba} & S_{Ca} \\ S_{Ab} & S_{Bb} & S_{Cb} \\ S_{Ac} & S_{Bc} & S_{Cc} \end{bmatrix} \begin{bmatrix} V_A \\ V_B \\ V_C \end{bmatrix} \quad (16)$$

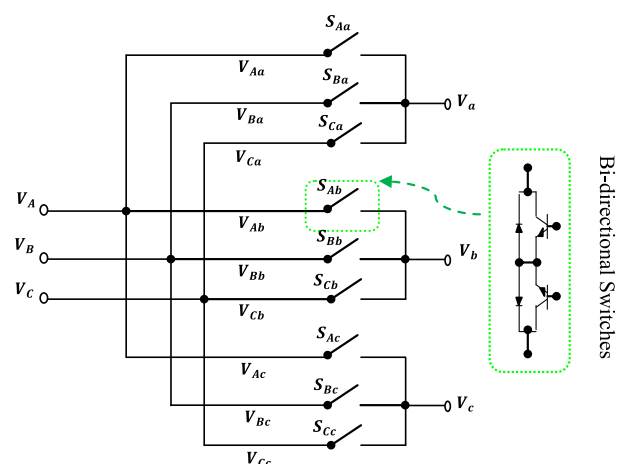


Fig. 7 – Matrix Converter structure.

The transfer matrix of MC is defined by the switching function (S_{jk}) as:

$$S_{jk} = \begin{cases} 1 \rightarrow S_{jk} \text{closed} & j \in \{A, B, C\}, k \in \{a, b, c\} \\ 0 \rightarrow S_{jk} \text{open} & \end{cases} \quad (17)$$

Knowing that the transfer matrix of calculating input currents is the transpose of the transfer matrix, in Eq. (16). The input currents (I_A , I_B , I_C) can also be calculated in terms of output currents (I_a , I_b , I_c) as:

$$\begin{bmatrix} I_A \\ I_B \\ I_C \end{bmatrix} = \begin{bmatrix} S_{Aa} & S_{Ab} & S_{Ac} \\ S_{Ba} & S_{Bb} & S_{Bc} \\ S_{Ca} & S_{Cb} & S_{Cc} \end{bmatrix} \begin{bmatrix} I_a \\ I_b \\ I_c \end{bmatrix} \quad (18)$$

Calculation time of each output phase voltage t_{jk} is a fraction of the switching frequency period T_s .

$$t_{jk} = S_{jk} \cdot T_s \quad (19)$$

with. $\sum t_{ja} = \sum t_{jb} = \sum t_{jc} = T_s$

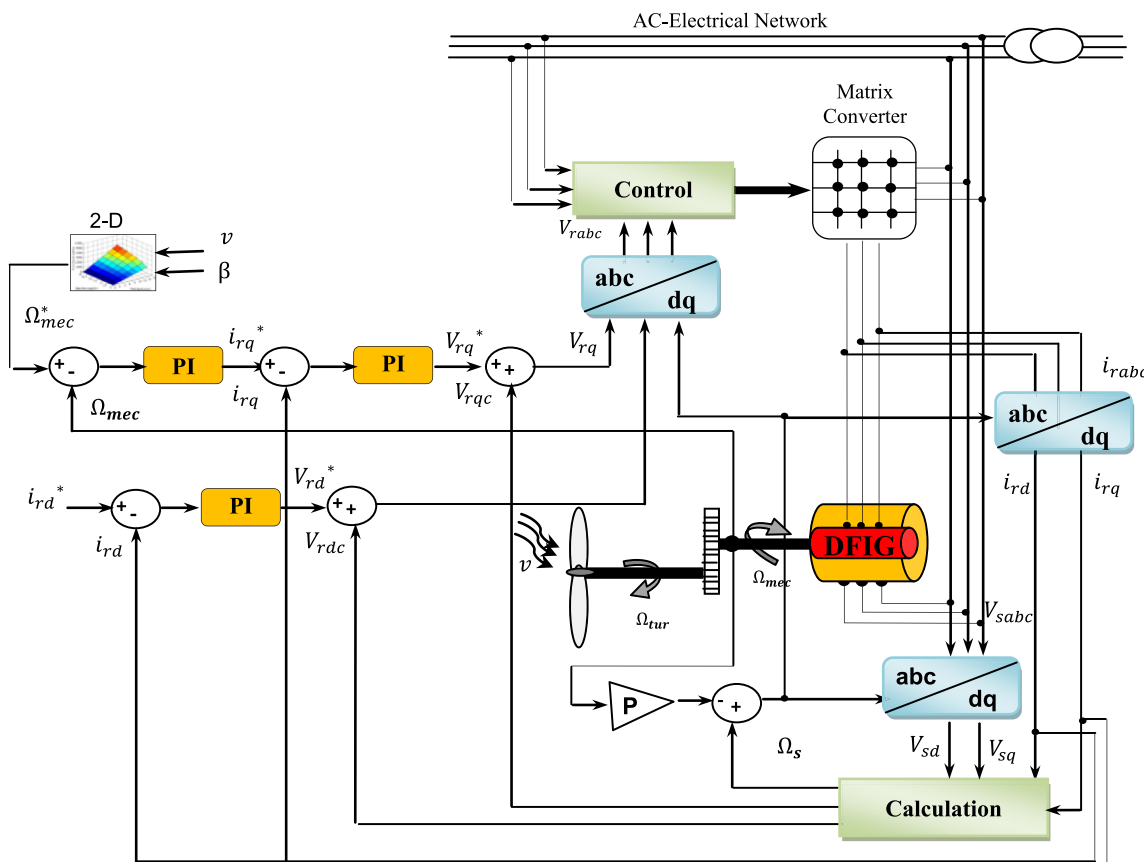


Fig. 8 – Control structure of wind turbine fed by matrix converter.

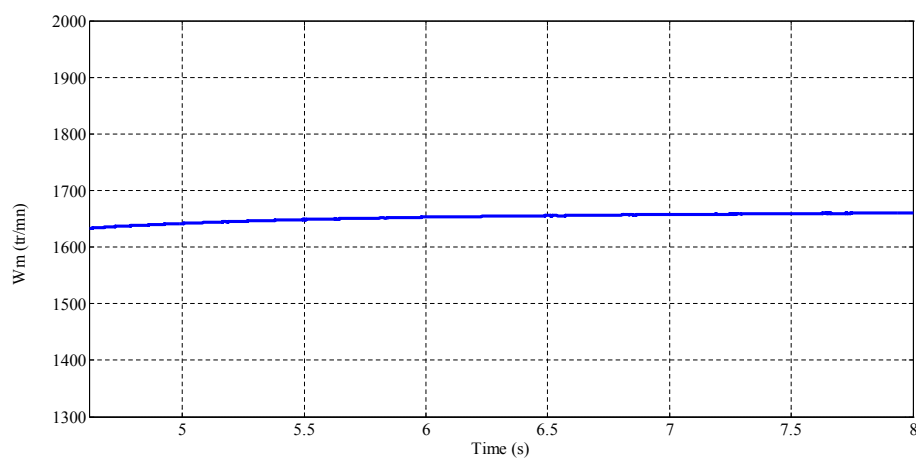


Fig. 9 – Speed machine.

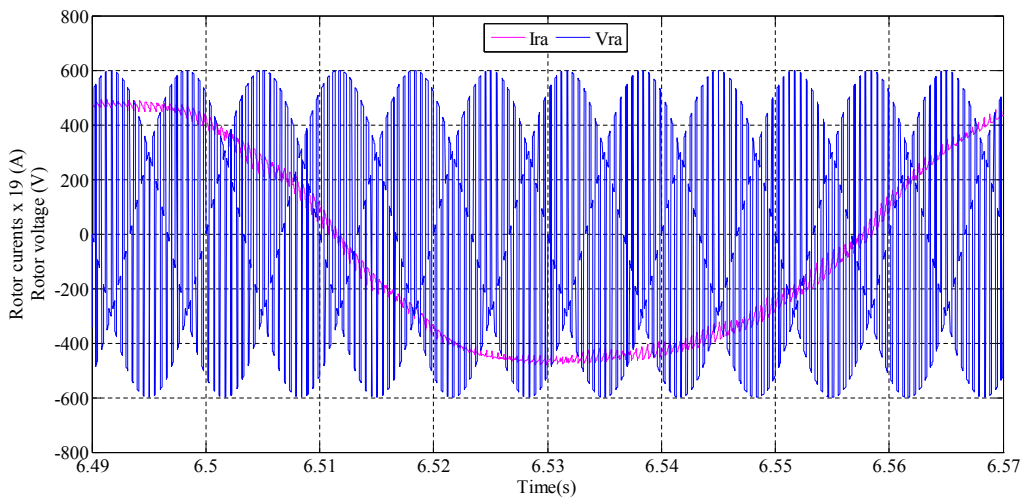


Fig. 10 – Output voltage and current waveforms of MC.

To eliminate open circuit to the output terminals or short circuit between input terminals, the switching constraint is defined as follow:

$$\sum S_{ja} = \sum S_{jb} = \sum S_{jc} = 1 \quad (20)$$

Taking into account the Venturini algorithm, he is defined of the three place input (V_A , V_B , V_C) and output (V_a , V_b , V_c) voltages at each sampling instant and is convenient for closed loop operations.

$$q = \sqrt{\frac{V_{os}^2}{V_{is}^2}} \quad (21)$$

The maximum ratio between output and the input voltage is 86,6% [12].

Based on Eqs. (20) and (21) matrix transfer can be calculated by the following three equations:

$$S_{jk} = \frac{1}{3} + \frac{2}{3} \frac{V_j V_k}{V_{is}^2} + \frac{2}{9} \frac{q}{q_s} \sin(\omega_i t + \phi_j) \cdot \sin(3\omega_i t) \quad (22)$$

$$V_j = V_{is} \cos(\omega_i t + \phi_j) \quad (23)$$

The desired output voltage is done by:

$$V_d = q V_{is} \cos(\theta_o + \theta_d) - \frac{q}{6} V_{is} \cos(3\theta_o) + \frac{1}{4} \frac{q}{q_s} V_{is} \cos(3\theta_i t) \quad (24)$$

Furthermore, V_{is} and θ_i is given in function of the measured V_{BC} and V_{AB} in the following form [22]:

$$V_{is}^2 = \frac{4}{9} (V_{AB}^2 + V_{BC}^2 + V_{AB} \cdot V_{BC}) \quad (25)$$

$$\theta_i = \arctan\left(\frac{V_{BC}}{\sqrt{3}\left(\frac{2}{3}V_{AB} + \frac{1}{3}V_{BC}\right)}\right) \quad (26)$$

So, we can write V_{os} and θ_o as:

$$V_{os} = \frac{2}{3} (V_a^2 + V_b^2 + V_c^2) \quad (27)$$

$$\theta_o = \arctan\left(\frac{V_b - V_c}{\sqrt{3}V_a}\right) \quad (28)$$

Control structure

From Eq. (13), it notices that the active and reactive stator powers can be controlled by means of the DFIG current i_{rq} and

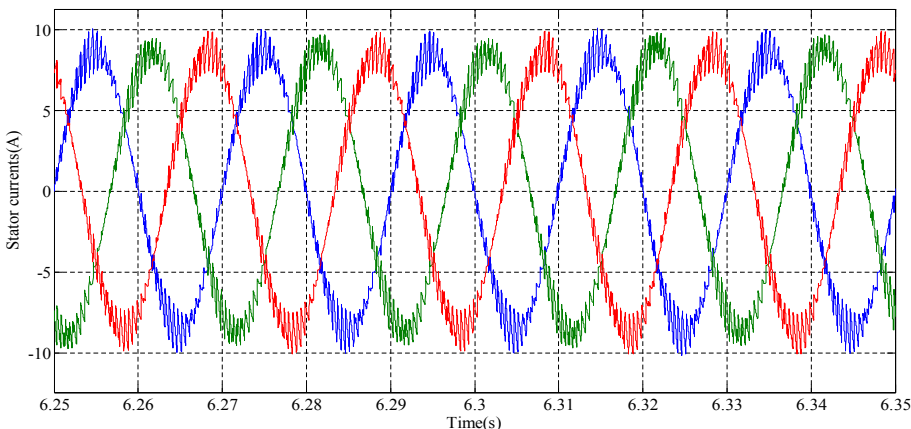


Fig. 11 – Three-phase stator currents.

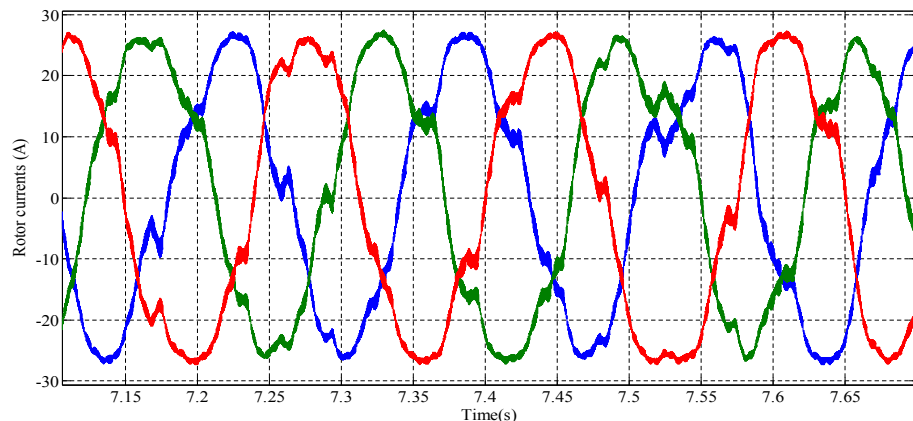


Fig. 12 – Three-phase rotor currents.

i_{rd} , respectively. Indeed, the model of DFIG in d-q reference frame with stator field orientation shows that the rotor currents can be controlled independently. The control structure of the wind conversion system based on DFIG fed by matrix converter is presented in Fig. 8.

In this section, two control loops are presented: control loop of the aero-turbine and control loop of the electric

generator via matrix converter. In effect, we firstly aim to extract maximum turbine power from the wind speed and the pitch angle control. So, 2-D lookup table is used to predict C_{opt} and λ_{opt} at which the turbine power reaches its maximum value. The 2-D lookup table provides the reference speed (Ω_{mec}^*) of the second loop. Furthermore, the rotor currents can be calculated independently. The current i_{rq}^* is calculated from

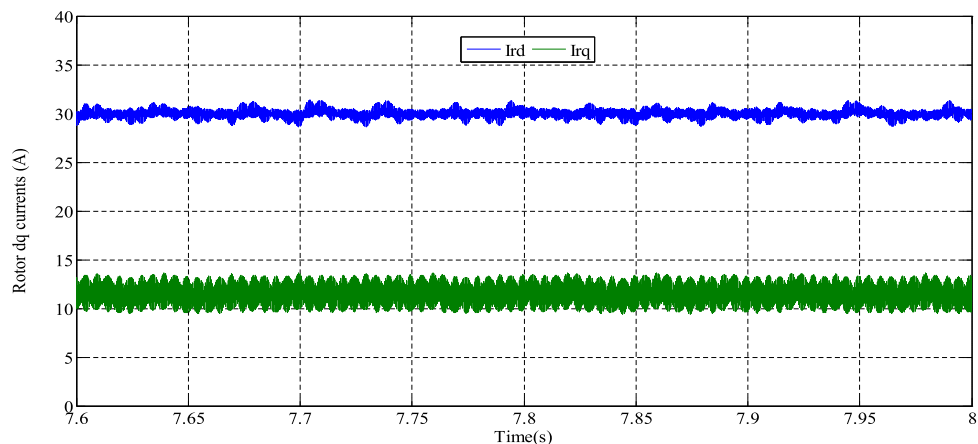


Fig. 13 – Direct and quadrature rotor currents.

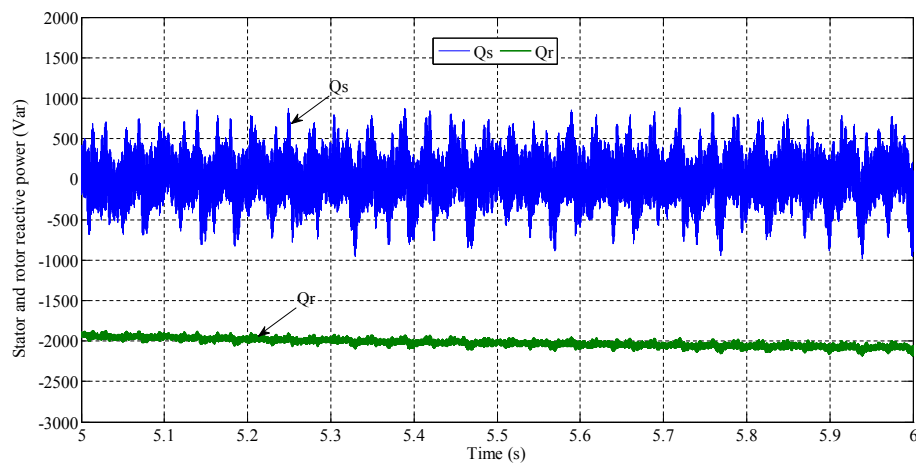


Fig. 14 – Rotor and stator reactive powers.

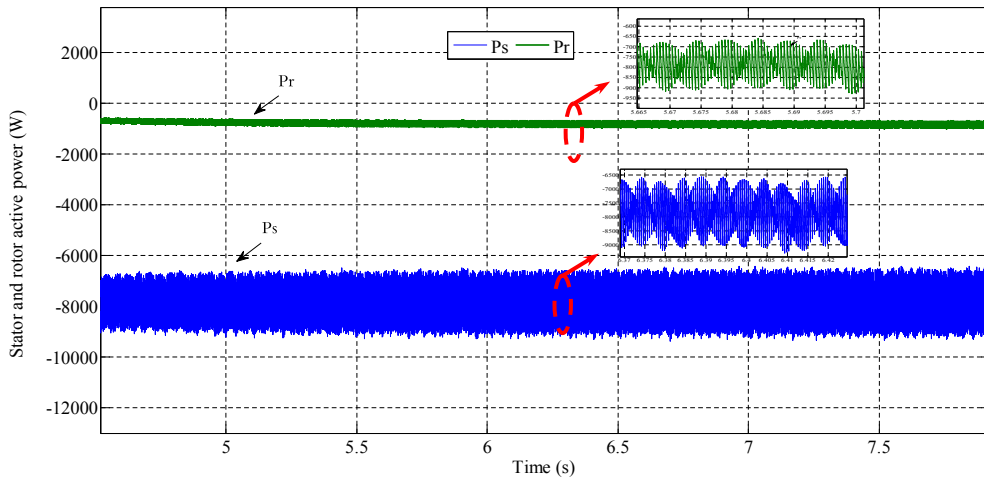


Fig. 15 – Rotor and stator active powers.

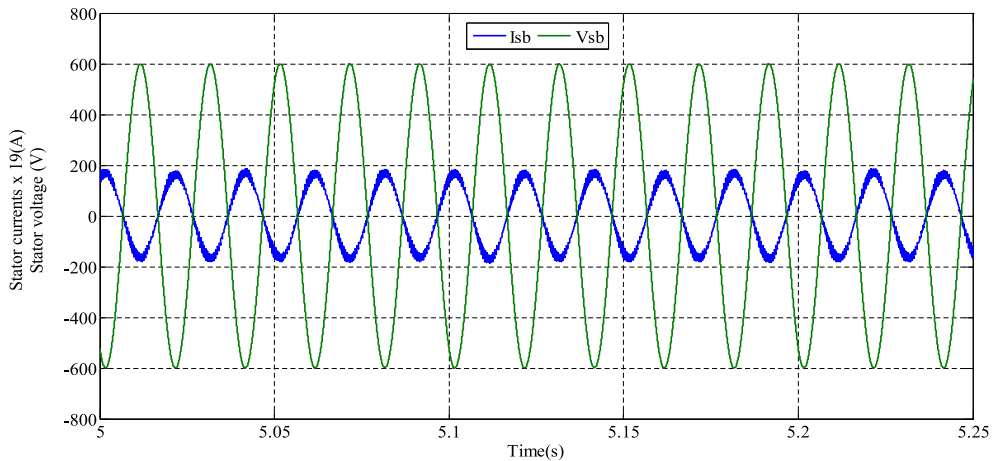


Fig. 16 – Stator voltage and current.

the speed control, and to get unity power factor in the connection of the MC with the grid we must setting $Q_{s_ref} = 0$. In effect, i_{rd}^* is given by the equation bellow:

$$i_{rd}^* = \frac{\varphi_{sd}}{M} - \frac{L_s}{M \cdot V_{sq}} \cdot Q_{s_ref} \quad (29)$$

Simulation results

In order to analyze the performance and feasibility of the system, the studied system is simulated using MatLab/Simulink software. The simulation results of the proposed study are shown in Figs. 9–15. Indeed, the wind profile considered in simulations under constant wind speed corresponding at rotational speed of the machine 1655rd/mn as shown by the Fig. 9 and the switching frequency has been chosen as 2 KHz.

In this condition, the waveforms of the voltage (V_{ra}) and current (i_{ra}) rotor are illustrated in Fig. 10. The voltage is that which is synthesized at the output of matrix converter fed double fed induction generator. Otherwise, Figs. 11 and 12 show, respectively, the stator and rotor currents and Fig. 13 shows the direct and quadrature rotor currents.

Here one can observe that the wind system works with a unity power factor whereby stator reactive power $Q_{s_ref} = 0$. In point of fact, Fig. 14 shows the zoom of the simulation results for the proposed direct power control strategy of DFIG based WECS, the rotor and stator reactive powers are given as 2 KVar and 0KVar, respectively. Also, Fig. 15 presents the active stator power (Ps) and active rotor power (Pr). Finally, the shape of the voltage and the current of a stator phase are given in Fig. 16. It observes a very good synchronization of these two quantities.

Conclusion

In this paper, the modeling and control of wind conversion system based on DFIG fed by matrix converter has been considered. The fact of the control of these powers separately permits to adjust the power factor of the installation and in consequence obtain better performance. The model of wind conversion chain is developed and the technique of maximum power point tracking has been applied to provide all of the active power generated to the grid with unity power factor. The simulation results showed that the active and reactive power of the wind energy present a high quality.

Nomenclature

P_s, Q_s	stator active and reactive power
P_r, Q_r	rotor active and reactive power
T_{em}	electromagnetic torque (N m)
d, q	synchronous reference frame index
V_{sd-q}	stator d–q frame voltage
V_{rd-q}	rotor d–q frame voltage
i_{sd-q}	stator d–q frame current
i_{rd-q}	rotor d–q frame current
φ_{sd-q}	stator d–q frame flux
φ_{rd-q}	rotor d–q frame flux
R_s, R_r	stator and rotor resistances
L_s, L_r	stator and rotor self inductances
M	mutual inductance
ω_s, ω_r	synchronous and rotor angular frequency
ρ	air density
V	wind speed
R	rotor radius
λ	tip-speed ratio
Ω_{tur}	aeroturbine rotor speed
Ω_m	generator speed
G	gearbox ratio
J	turbine total inertia
σ	coefficient of dispersion
q	demand voltage ratios
V_{is}	peak input voltage
ω_i	angular frequencies of input voltage
ω_o	angular frequencies of output voltage

Appendix

Font Simulated DFIG Wind Turbine Parameters:

$R_s = 0.435 \Omega$, $R_r = 0.62 \Omega$, $L_s = 0.084 \text{ H}$, $L_r = 0.081 \text{ H}$, $M = 0.078 \text{ H}$, Number of pole pairs $P = 2$, $J = 0.35 \text{ kgm}^2$, $F = 6.73e^{-3} \text{ N.m.s.}$, $R = 3 \text{ m}$, $\rho = 1.25 \text{ kg/m}^3$, $G = 12.3$, $f = 50 \text{ Hz}$.

REFERENCES

- [1] The renewable energies website. Available: <http://www.les-energies-renouvelables.eu/avantages-et-inconvénients-de-l'énergie-eolienne.html>
- [2] Lu MS, Chang CL, Lee WJ, Wang L. Combining the wind power generation system with energy storage equipment. *IEEE Trans Ind Appl* 2009;45:2109–15.
- [3] Wenyi L, Baoping T, Yonghua J. Status and problems of wind turbine structural health monitoring techniques in China: review. *Renew Energy* 2010;35:1414–8.
- [4] World Wind Energy Report. WWEA (World Wind Energy Association). 2008.
- [5] Bedoud K, Alirachedi M, Bahi T, Lakel F, Grid A. Robust control of doubly fed induction generator for wind turbine under sub-synchronous operation mode. *Energy Procedia* 2015;74:886–99.
- [6] Cheng M, Zhu Y. The state of the art of wind energy conversion systems and technologies: a review. *Energy Convers Manag* 2014;88:332–47.
- [7] Khalfallah T, Belfadal C, Allaoui T, Champenois G. Power control of wind turbine based on fuzzy sliding mode control. *Int J Power Electron Drive Syst (IJPEDS)* 2015;5(4):502–11.
- [8] Blaabjerg F, Iov F, Chen Z, Ma K. Power electronics and controls for wind turbine systems. *IEEE Int Energy Conf Exhib* 2010:333–44.
- [9] Altun H, Sunter S. Matrix converter induction motor drive: modeling, simulation and control. *Electr Eng* 2003;86:25–33.
- [10] Abdel-Rahim O, Abu-Rub H, Kouzou A. Nine-to-three phase direct matrix converter with model predictive control for wind generation system. *Energy Procedia* 2013;42:173–82.
- [11] Afonso LFP. Maximum power point tracker of wind energy generation systems using matrix converters. Portugal: Memory for graduating from Master's degree in Electrical and Computer Engineering, Higher Technical Institute, Technical University of Lisbon; 2011.
- [12] Hamane B, Doumbia ML, Bouhamida M, Chaoui H, Benghanem M. Modeling and control of a wind energy conversion system based on DFIG driven by a matrix converter. In: IEEE Eleventh International Conference on Ecological Vehicles and Renewable Energies (EVER); 2016.
- [13] Bedoud K, Alirachedi M, Bahi T, Lakel F. Adaptive fuzzy gain scheduling of PI controller for control of the wind energy conversion systems. *Energy Procedia* 2015;74:211–25.
- [14] Senju T, Sakamoto R, Urasaki N, Funabashi T, Sekine H. Output power leveling of wind farm using pitch angle control with fuzzy neural network. In: IEEE power electron conf; 2006. <http://dx.doi.org/10.1109/PES.2006.1709377>. IEEE Xplore: 16 October 2006, ISBN: 1-4244-0493-2, ISSN: 1932-5517.
- [15] Ramtharan G, Ekanayake JB, Jenkins N. Frequency support from doubly fed induction generator wind turbines. *IET Renew Power Gener* 2007;1(1):3–9.
- [16] Morimoto S, Nakayama H, Sanada M, Takeda Y. Sensorless output maximization control for variable-speed wind generation system using IPMSG. *IEEE Trans Ind Appl* 2005;41(1):60–7.
- [17] Zhang J, Cheng M, Chen Z, Fu X. Pitch angle control for variable speed wind turbines. 2008, 6–9 April. DRPT2008, Nanjing China.
- [18] Barambones O, Jose M, Gonzalez D, Kremers E. Adaptive robust control to maximizing the power generation of a variable speed wind turbine. In: International Conference on Renewable Energy Research and Applications Madrid. Spain: IEEE, ICRERA; 2013, 20–23 October. p. 167–72.
- [19] Beltran B, Sliding, al. Mode power control of variable speed wind energy conversion systems. *IEEE Trans Energy Convers* 2008;23:551–8.
- [20] Fernando, D.B., Hrman D. B., & Ricardo J. M. Wind turbine control systems advances in industrial control series. Springer.
- [21] Abdeddaim S, Betka A. Optimal tracking and robust power control of the DFIG wind turbine. *Electr Power Energy Syst* 2013;49:234–42.
- [22] Hüseyin A, Sedat S. Modeling, simulation and control of wind turbine driven doubly-fed induction generator with matrix converter on the rotor side. *Electr Eng* 2013;95:157–70.
- [23] Hector A, Painemal P, Sauer PW. Power system modal analysis considering doubly-fed induction generators. In: Proceedings of IEEE-IREP'10, Buzios, RJ, Brazil; 2010.
- [24] Gaillard A. Wind system based on the DFIG: contribution to the study of the quality of the electric energy and the continuity of service. Doct. thesis. France: Henri Poincaré University, Nancy-I; 2010.
- [25] Kassem AM, Hasaneen KM, Yousef Ali M. Dynamic modeling and robust power control of DFIG driven by wind turbine at infinite grid. *Electr Power Energy Syst* 2013;44:375–82.
- [26] Wheeler P, Rodriguez J, Clare JC, Empringham L, Weintein A. Matrix converters a technology review ». *IEEE Trans Ind Electr* 2002;49:276–88.

- [27] Shapoval I, Clare J, Chekhet E. Experimental study of a matrix converter excited doubly-fed induction machine in generation and motoring. In: 13th international power electronics and motion control conference (EPE-PEMC); 2008. p. 307–12.
- [28] Sherif MD, Abdel-khalik A, Shehab A, Massoud A. Performance of a three-to-five matrix converter fed five-phase induction motor under open-circuit switch faults. In: IEEE symp comp appl ind electron; 2016. <http://dx.doi.org/10.1109/ISCAIE.2016.7575056>.